4.5.5 Yield criteria based on plasticity theory

More complex functions also include the third invariant of the deviator stress tensor $J_3 = S_1 S_2 S_3$. For example, Desai and Salami (1987) were able to obtain excellent fits to peak strength (assumed synonymous with yield) and stress-strain data for a sandstone, a granite and a dolomite using the yield function

$$F = J_2 - \left(\frac{\alpha}{\alpha_0^{n-2}} I_1^n + I_1^2 \right) \left(1 - \beta \frac{J_3^{1/3}}{J_2^{1/2}} \right)^m$$

where α , β , m and n are material parameters and α_0 is one unit of stress.

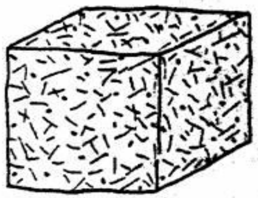

random → isotropic

e.g. igneous and sedimentary rocks

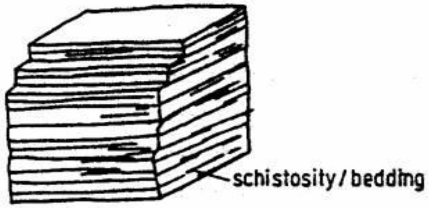

planar → transversely isotropic

e.g. metamorphic and sedimentary rocks

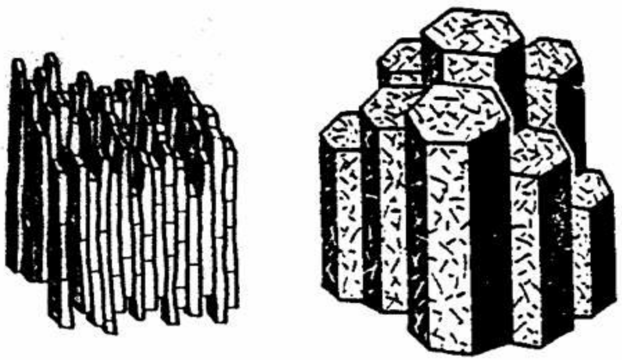

linear → transversely isotropic

e.g. metamorphic rocks

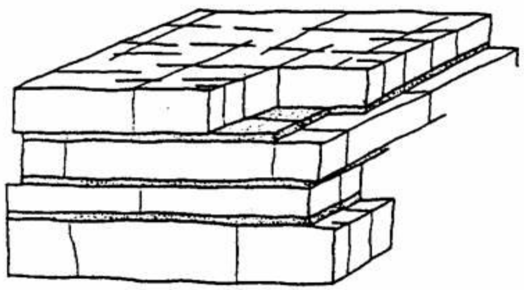

3 orthogonal weakness → orthotropic

- 試解釋或說明下列各項：**(91專技)**

  指出**Orthotropic material**與**Transversely isotropic material**有何不同？**(10分)**

- 試解釋或回答下列各項：**(87專技)**

  何謂強度異向性（**Strength anisotropy**）？試列舉二種有顯著強度異向性之岩石？**(6分)**

TABLE 4.1 Relationships Among Elastic Moduli E, G, K, ν, λ, M

Isotropic Material

	Shear Modulus, G	Young's Modulus, E	Constrained Modulus, M	Bulk Modulus, K	Lame Parameter, λ	Poisson's Ratio, ν
G, E	G	E	$\frac{G(4G-E)}{3G-E}$	$\frac{GE}{9G-3E}$	$\frac{G(E-2G)}{3G-E}$	$\frac{E-2G}{2G}$
G, M	G	$\frac{G(3M-4G)}{M-G}$	M	$M-\frac{4}{3}G$	$M-2G$	$\frac{M-2G}{2(M-G)}$
G, K	G	$\frac{9GK}{3K+G}$	$K+\frac{4}{3}G$	K	$K-\frac{2G}{3}$	$\frac{3K-2G}{2(3K+G)}$
G, λ	G	$\frac{G(3\lambda+2G)}{\lambda+G}$	$\lambda+2G$	$\lambda+\frac{2G}{3}$	λ	$\frac{\lambda}{2(\lambda+G)}$
G, ν	G	$2G(1+\nu)$	$\frac{2G(1-\nu)}{1-2\nu}$	$\frac{2G(1+\nu)}{3(1-2\nu)}$	$\frac{2G\nu}{1-2\nu}$	ν
E, K	$\frac{3KE}{9K-E}$	E	$\frac{K(9K+3E)}{9K-E}$	K	$\frac{K(9K-3E)}{9K-E}$	$\frac{3K-E}{6K}$
E, ν	$\frac{E}{2(1+\nu)}$	E	$\frac{E(1-\nu)}{(1+\nu)(1-2\nu)}$	$\frac{E}{3(1-2\nu)}$	$\frac{\nu E}{(1+\nu)(1-2\nu)}$	ν
K, λ	$\frac{3(K-\lambda)}{2}$	$\frac{9K(K-\lambda)}{3K-\lambda}$	$3K-2\lambda$	K	λ	$\frac{\lambda}{3K-\lambda}$
K, M	$\frac{3(M-K)}{4}$	$\frac{9K(M-K)}{3K+M}$	M	K	$\frac{3K-M}{2}$	$\frac{3K(2M-1)+M}{3K(2M+1)-M}$
K, ν	$\frac{3K(1-2\nu)}{2(1+\nu)}$	$3K(1-2\nu)$	$\frac{3K(1-\nu)}{1+\nu}$	K	$\frac{3K\nu}{1+\nu}$	ν

transversely isotropic

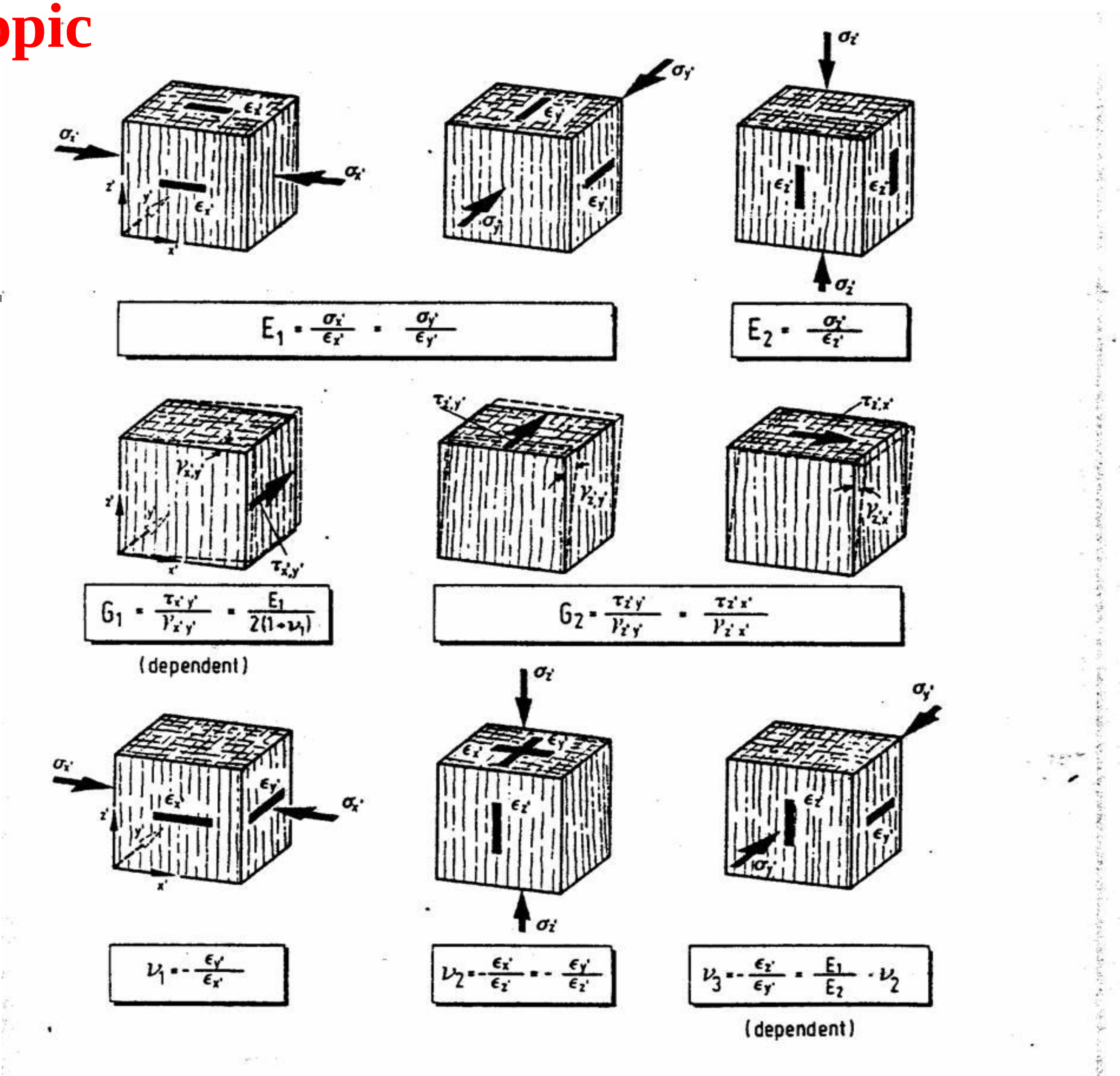

Fig. 3.14. Definition of elastic constants for the case of transverse isotropy and linear fabric in terms of stresses and both normal and shear strains in a three-dimensional element.

orthotropic

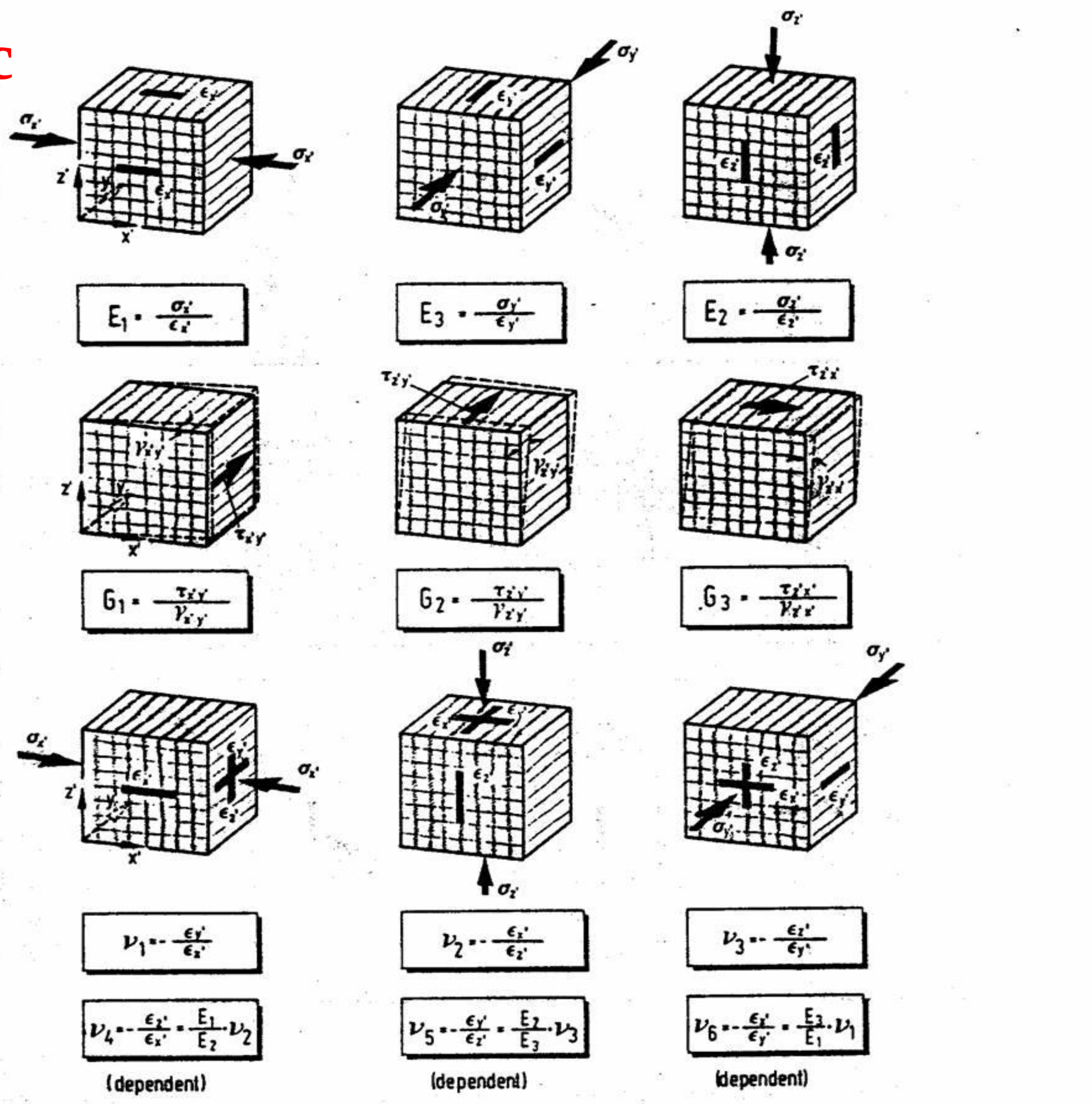

Fig. 3.15. Definition of the elastic constants in the case of orthotropy in terms of stresses and both normal and shear strains in a three-dimensional element.

4.6 Strength of anisotropic rock material in triaxial compression

Because of some preferred orientation of the fabric or microstructure, or the presence of bedding or cleavage planes, the behaviour of many rocks is anisotropic. Because of computational complexity and the difficulty of determining the necessary elastic constants, it is usual for only the simplest form of anisotropy, transverse isotropy, to be used in design analyses. Anisotropic strength criteria are also required for use in the calculations.

Figure 4.31 shows some measured variations in peak principal stress difference with the angle of inclination of the major principal stress to the plane of weakness.

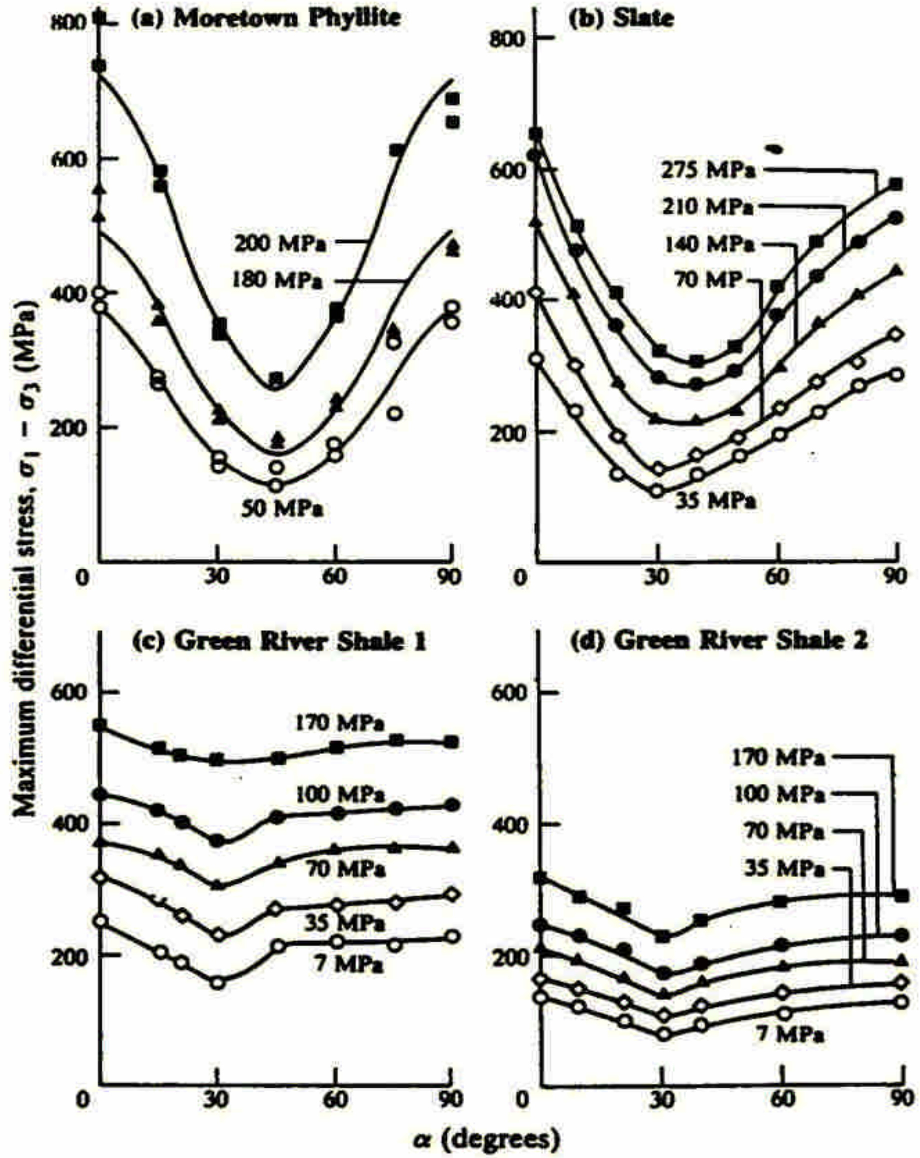

Figure 4.31 Variation of peak principal stress difference with the angle of inclination of the major principal stress to the plane of weakness, for the confining pressures indicated for (a) a phyllite (after Donath, 1972), (b–d) a slate and two shales (after McLamore and Gray, 1967).

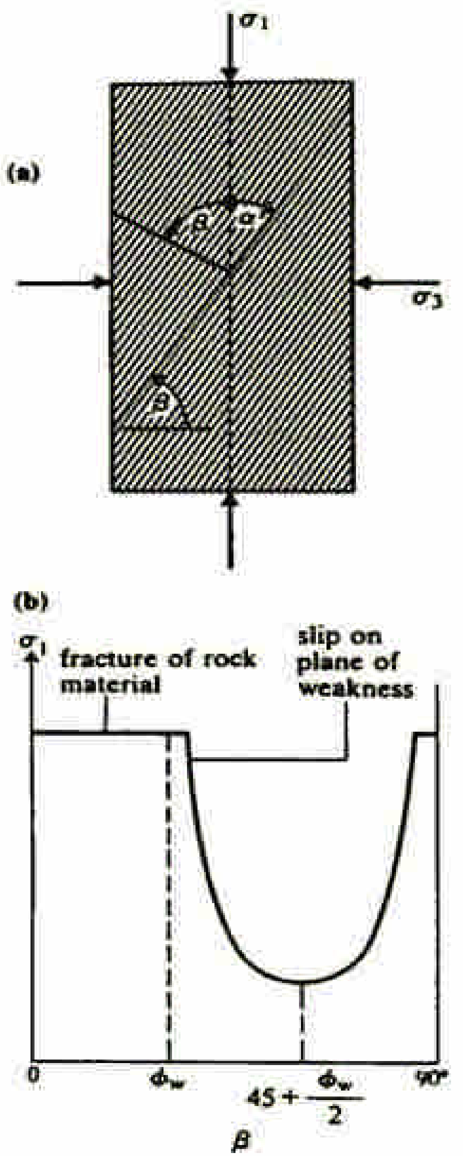

Figure 4.32 (a) Transversely isotropic specimen in triaxial compression. (b) variation of peak strength at constant confining pressure with the angle of inclination of the normal to the plane of weakness to the compression axis (β).

4.6 Strength of anisotropic rock material in triaxial compression

Jaeger (1960) introduced an instructive analysis of the case in which the rock contains well-defined, parallel planes of weakness whose normals are inclined at an angle β to the major principal stress direction as shown in Figure 4.32a. Each plane of weakness has a limiting shear strength defined by Coulomb's criterion

$$S = C_w + \sigma_n \tan \phi_w \qquad \textbf{(4.28)}$$

4.6 Strength of anisotropic rock material in triaxial compression

Slip on the plane of weakness (*ab*) will become incipient when the shear stress on the plane, τ , becomes equal to, or greater than, the shear strength, s . The stress transformation equations give the normal and shear stresses on *ab* as

$$\sigma_n = \frac{1}{2}(\sigma_1 + \sigma_3) + \frac{1}{2}(\sigma_1 - \sigma_3)\cos 2\beta$$

and

$$\tau = \frac{1}{2}(\sigma_1 - \sigma_3)\sin 2\beta \qquad \textbf{(4.29)}$$

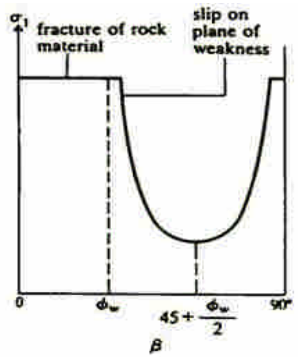

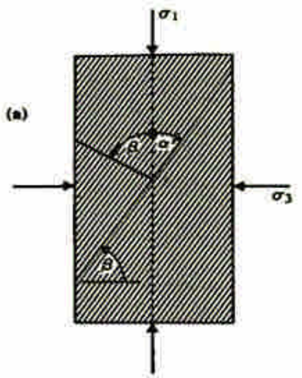

Figure 4.32 (a) Transversely isotropic specimen in triaxial compression; (b) variation of peak strength at constant confining pressure with the angle of inclination of the normal to the plane of weakness to the compression axis (β).

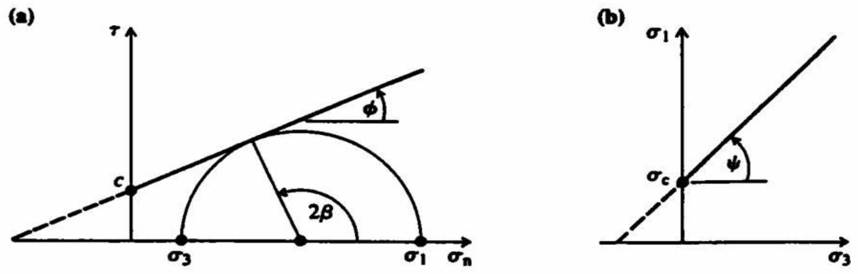

Figure 4.23 Coulomb strength envelopes in terms of (a) shear and normal stresses, and (b) principal stresses.

$$S = C_w + \sigma_n \tan \phi_w \qquad \textbf{(4.28)}$$

4.6 Strength of anisotropic rock material in triaxial compression

Substituting for σ_n in equation. 4.28, putting $s = \tau$ and rearranging, give the criterion for slip on the plane of weakness as

$$(\sigma_1 - \sigma_3)_s = \frac{2(c_w + \sigma_3 \tan \phi_w)}{(1 - \tan \phi_w \cot \beta)\sin 2\beta} \qquad \textbf{(4.30)}$$

The principal stress difference required to produce slip tends to infinity as $\beta \to 90^\circ$ and as $\beta \to \phi_w$（分母為零）

4.6 Strength of anisotropic rock material in triaxial compression

By differentiation, it is found that the minimum strength occurs when (將4.30對 β 微分，並令爲O)

Drive & Memorize.

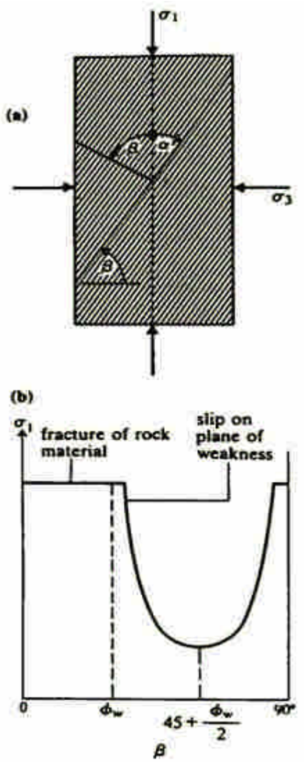

Figure 4.32 (a) Transversely isotropic specimen in triaxial compression: (b) variation of peak strength at constant confining pressure with the angle of inclination of the normal to the plane of weakness to the compression axis (β).

$$(\sigma_1 - \sigma_3)_s = \frac{2(c_w + \sigma_3 \tan\phi_w)}{(1 - \tan\phi_w \cot\beta)\sin 2\beta} \qquad \textbf{(4.30)}$$

$$\tan 2\beta = -\cot\phi_w$$

or when

Drive & Memorize.

$$\beta = \frac{\pi}{4} + \frac{\phi_w}{2}$$

Homework

推導 $\beta = \frac{\pi}{4} + \frac{\phi_w}{2}$

The criterion for slip on the plane of weakness as

$$(\sigma_1 - \sigma_3)_s = \frac{2(c_w + \sigma_3 \tan \phi_w)}{(1 - \tan \phi_w \cot \beta)\sin 2\beta}$$

$$f = (\sigma_1 - \sigma_3)_s = \frac{2(c_w + \sigma_3 \tan \phi_w)}{(1 - \tan \phi_w \cot \beta)\sin 2\beta}$$

By partial differentiation $\frac{\partial f}{\partial \beta} = 0$

$$f = (\sigma_1 - \sigma_3)_s = \frac{2(c_w + \sigma_3 \tan\phi_w)}{(1 - \tan\phi_w \cot\beta)\sin 2\beta}$$

$$\frac{\partial f}{\partial \beta} = \frac{-2(c_w + \sigma_3 \tan\phi_w)[(1 - \tan\phi_w \cot\beta)\sin 2\beta]'}{[(1 - \tan\phi_w \cot\beta)\sin 2\beta]^2} = 0$$

Gives

$$\frac{\partial[(1 - \tan\phi_w \cot\beta)\sin 2\beta]}{\partial\beta} = 0$$

$$2\cos 2\beta + \tan\phi_w (2\sin 2\beta) = 0$$

$$\tan 2\beta = -\cot\phi_w$$

$$\beta = \frac{\pi}{4} + \frac{\phi_w}{2}$$

4.6 Strength of anisotropic rock material in triaxial compression

For Intact Rock

$$\sigma_1 = \frac{2c\cos\phi + \sigma_3(1+\sin\phi)}{1-\sin\phi} \quad \textbf{(4-14)}$$

or

$$\sigma_1 = \sigma_3 K_p + 2c\sqrt{K_p}$$

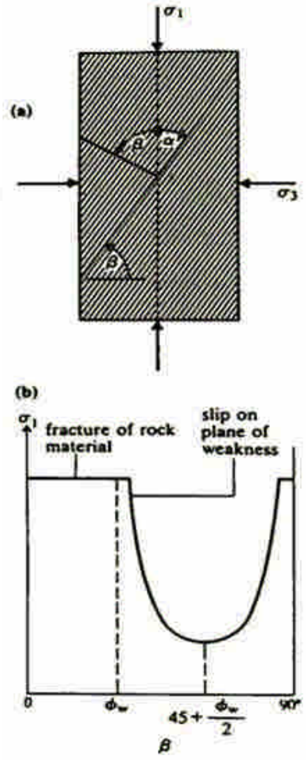

Figure 4.32 (a) Transversely isotropic specimen in triaxial compression; (b) variation of peak strength at constant confining pressure with the angle of inclination of the normal to the plane of weakness to the compression axis (β).

4.6 Strength of anisotropic rock material in triaxial compression

The corresponding value of the principal stress difference

$$(\sigma_1 - \sigma_3)_{\min} = 2(c_w + \mu_w \sigma_3)\left(\left[1 + \mu_w^2\right]^{1/2} + \mu_w\right)$$

where $\mu_w = \tan\phi_w$

For values of β approaching 90° and in the range 0° to ϕ_w , slip on the plane of weakness cannot occur, and so the peak strength of the specimen for a given value of σ_3 must be governed by some other mechanism, probably shear fracture through the rock material in a direction not controlled by the plane of weakness.

4.6 Strength of anisotropic rock material in triaxial compression

Such observations led Jaeger (1960) to propose that the shear strength parameter, c_w , is not constant but is continuously variable with β or α . McLamore and Gray (1967) subsequently proposed that both c_w and $\tan\phi_w$, vary with orientation according to the empirical relations

$$c_w = A - B\left[\cos 2(\alpha - \alpha_{c0})\right]^n$$

and

$$\tan\phi_w = C - D\left[\cos 2(\alpha - \alpha_{\phi 0})\right]^m$$

where *A, B, C, D, m* and *n* are constants, and α_{c0} and $\alpha_{\phi 0}$ are the values of α at which c_w and ϕ_w take minimum values, respectively.

4.7 Shear behaviour of discontinuities
4.7.1 Shear testing

The most commonly used method for the shear testing of discontinuities in rock is the direct shear test. As shown in Figure 4.33.

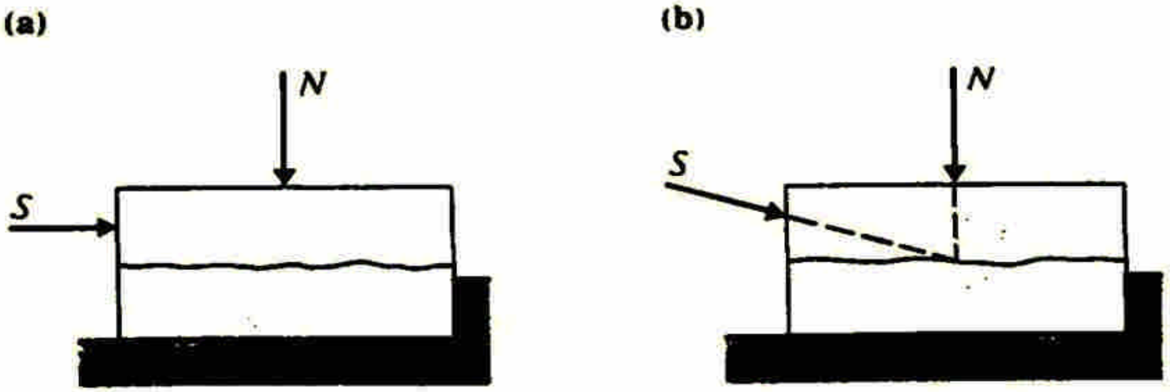

Figure 4.33 Direct shear test configurations with (a) the shear force applied parallel to the discontinuity, (b) an inclined shear force.

4.7 Shear behaviour of discontinuities

4.7.1 Shear testing

This type of test is commonly carried out in the laboratory, but it may also be carried out in the field, using a portable shear box to test discontinuities contained in pieces of drill core or as an in situ test on samples of larger size. Methods of preparing samples and carrying out these various tests are discussed by the ISRM Commission (1974), Goodman (1976) and Hoek and Bray (1981).

4.7 Shear behaviour of discontinuities
4.7.1 Shear testing

Figure 4.33a can cause a moment to be applied about a lateral axis on the discontinuity surface. This produces relative rotation of the two halves of the specimen and a non-uniform distribution of stress over the discontinuity surface.

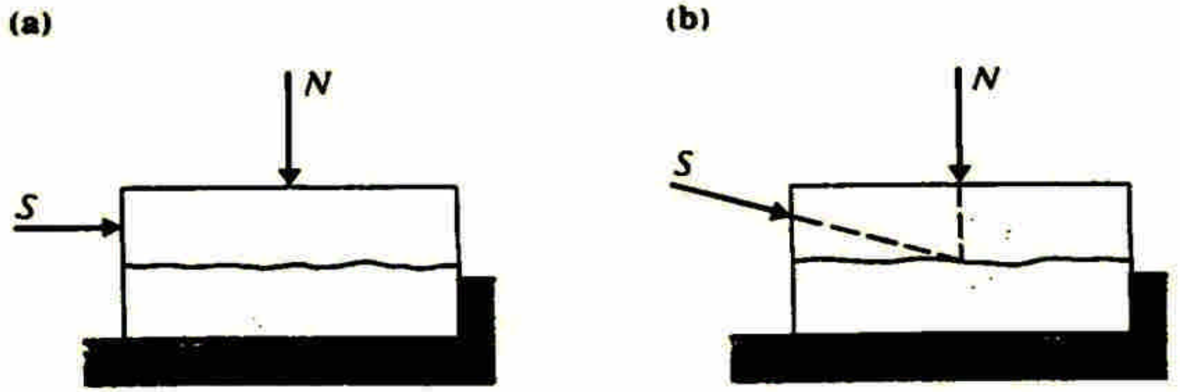

Figure 4.33 Direct shear test configurations with (a) the shear force applied parallel to the discontinuity, (b) an inclined shear force.

4.7 Shear behaviour of discontinuities

4.7.1 Shear testing

To minimise these effects, the shear force may be inclined at an angle (usually $10^\circ - 15^\circ$) to the shearing direction as shown in Figure 4.33b.

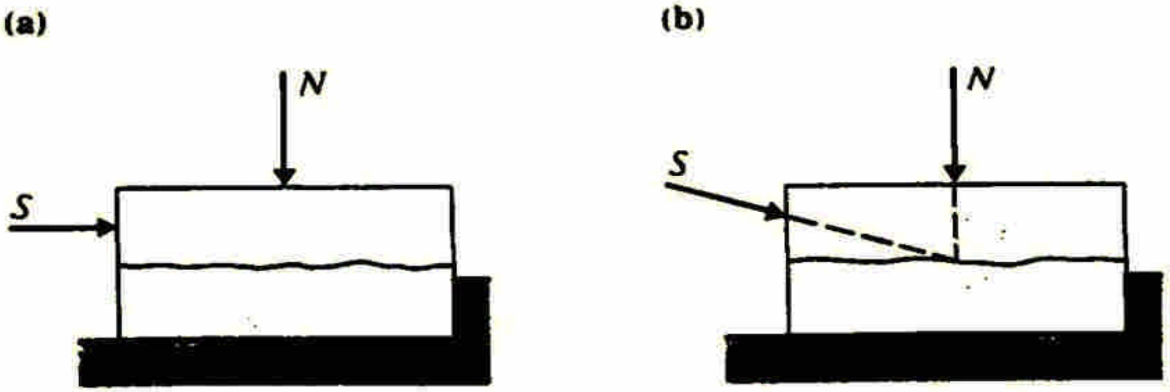

Figure 4.33 Direct shear test configurations with (a) the shear force applied parallel to the discontinuity, (b) an inclined shear force.

4.7 Shear behaviour of discontinuities
4.7.1 Shear testing

This is almost always done in the case of large-scale in situ tests. Because the mean normal stress on the shear plane increases with the applied shear force up to peak strength, it is not possible to carry out tests in this configuration at very Iow normal stresses.

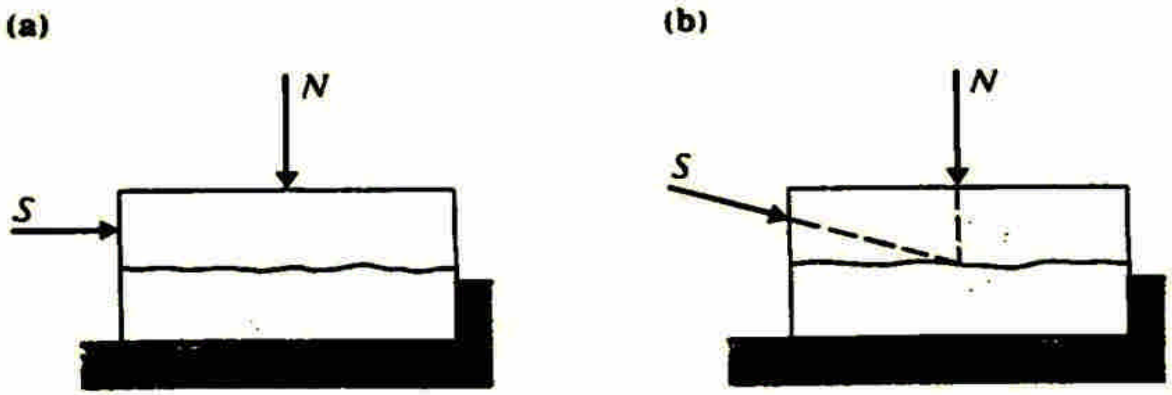

Figure 4.33 Direct shear test configurations with (a) the shear force applied parallel to the discontinuity, (b) an inclined shear force.

4.7 Shear behaviour of discontinuities
4.7.1 Shear testing

Undrained testing with the measurement of induced joint water pressures, is generally not practicable using the shear box.

4.7 Shear behaviour of discontinuities
4.7.1 Shear testing

The triaxial cell is sometimes used to investigate the shear behaviour of discontinuities. Specimens are prepared from cores containing discontinuities inclined at $25^\circ - 40^\circ$ to the specimen axis.

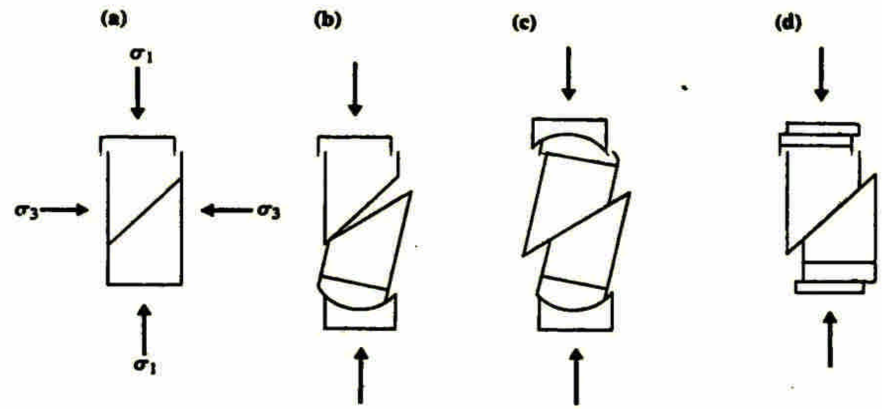

Figure 4.34 Discontinuity shear testing in a triaxial cell (after Jaeger and Rosengren, 1969).

4.7 Shear behaviour of discontinuities
4.7.1 Shear testing

The triaxial cell is well suited to testing discontinuities in the presence of water. Tests may be either drained or undrained, preferably with a known level of joint water pressure being imposed

and maintained throughout the test.

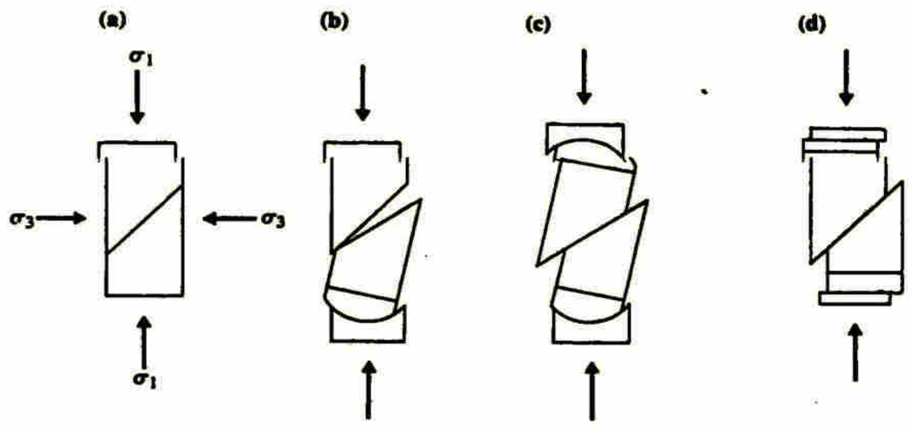

Figure 4.34 Discontinuity shear testing in a triaxial cell (after Jaeger and Rosengren, 1969).

4.7 Shear behaviour of discontinuities
4.7.1 Shear testing

If relative shear displacement of the two parts of the specimen is to occur, there must be lateral as well as axial relative translation.

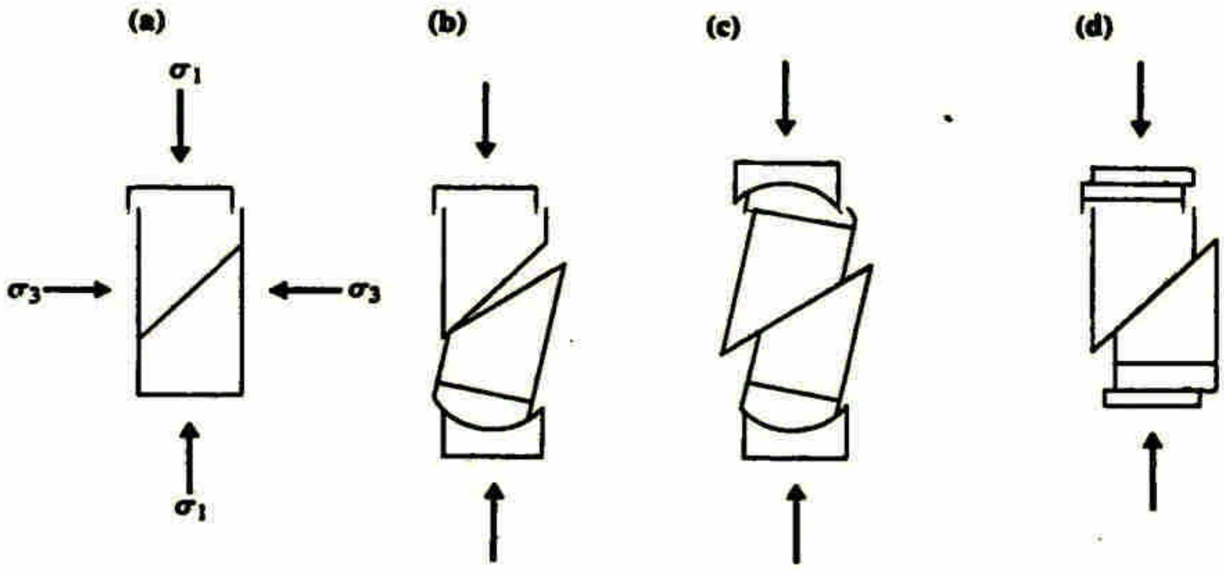

Figure 4.34 Discontinuity shear testing in a triaxial cell (after Jaeger and Rosengren, 1969).

4.7 Shear behaviour of discontinuities
4.7.1 Shear testing

A spherical seat is used in the system, axial displacement causes the configuration

to change to that of Figure 4.34b, which is clearly unsatisfactory.

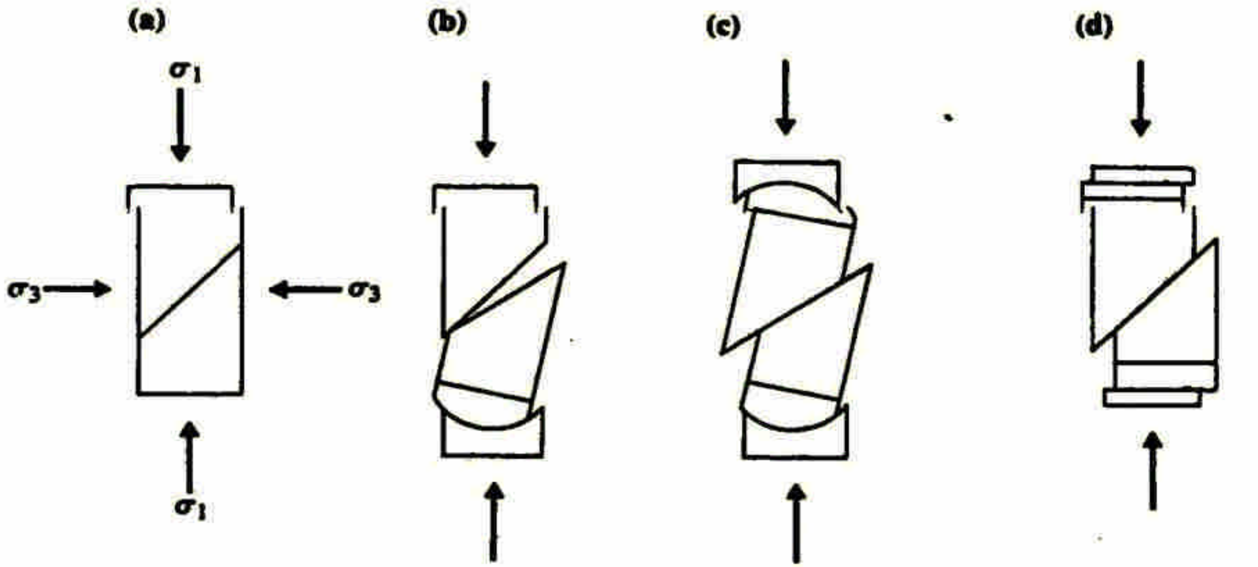

Figure 4.34 Discontinuity shear testing in a triaxial cell (after Jaeger and Rosengren, 1969).

4.7 Shear behaviour of discontinuities
4.7.1 Shear testing

Two spherical seats allows full contact to be maintained over the sliding surfaces, but the area of contact changes and frictional and lateral forces are introduced at the seats.

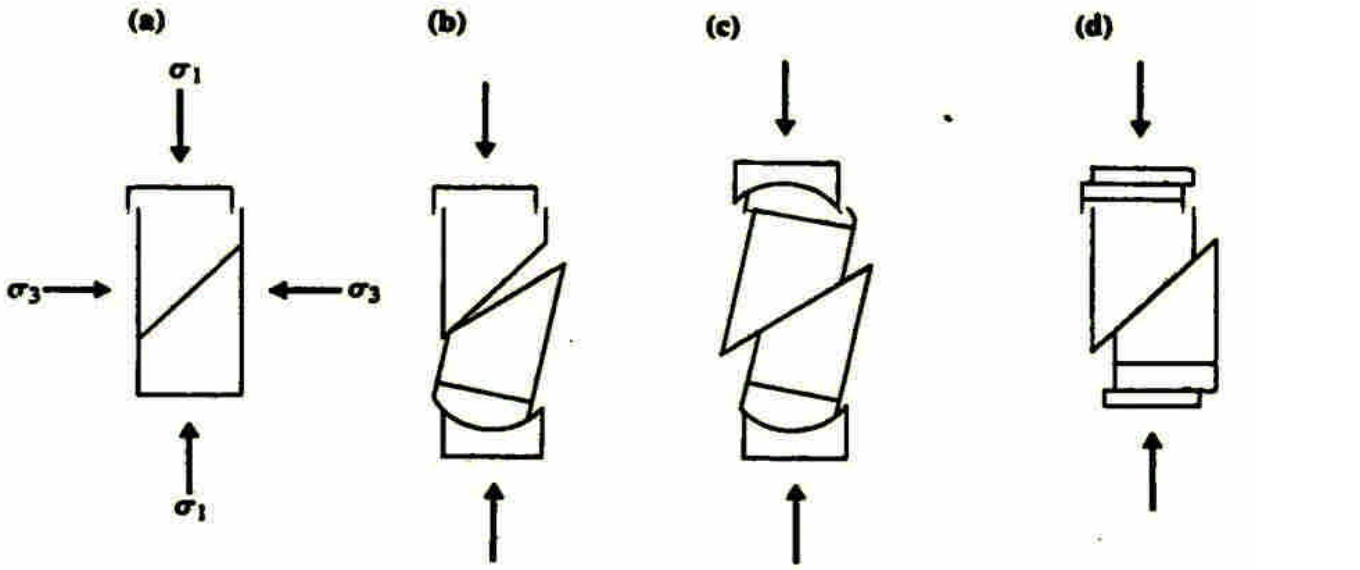

Figure 4.34 Discontinuity shear testing in a triaxial cell (after Jaeger and Rosengren, 1969).

4.7 Shear behaviour of discontinuities
4.7.1 Shear testing

Figure 4.34d illustrates the most satisfactory method of ensuring that the lateral component of translation can occur freely and that contact of the discontinuity surfaces is maintained. Pairs of hardened steel discs are inserted between the platens and either end of the specimen. No spherical seats are used.

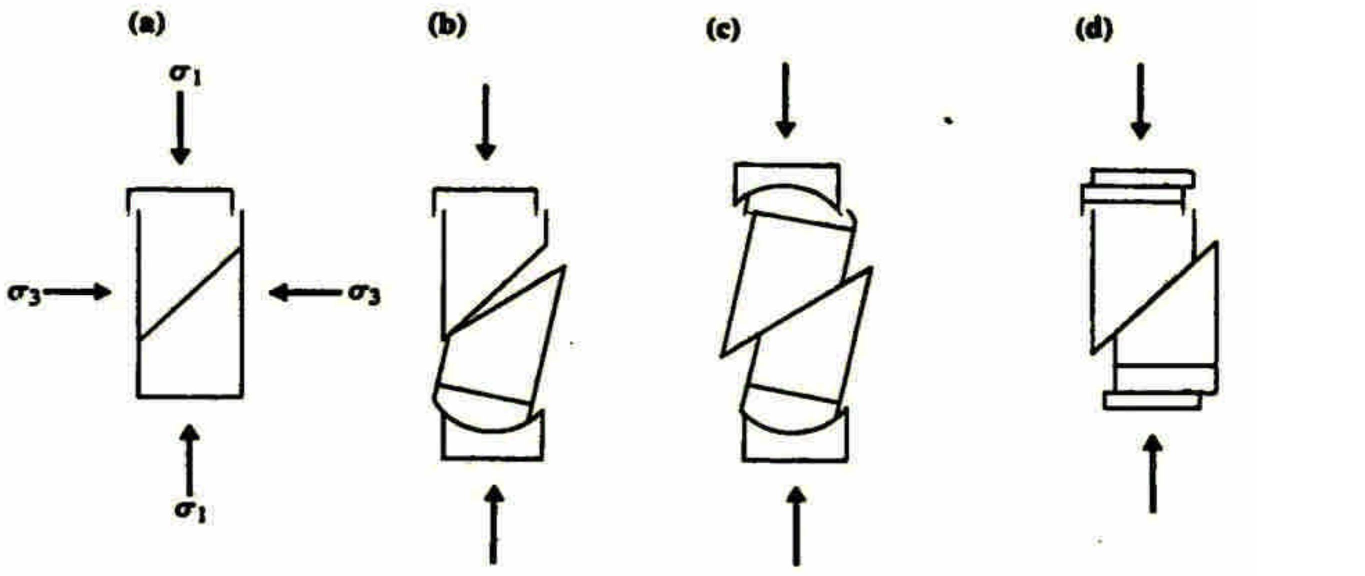

Figure 4.34 Discontinuity shear testing in a triaxial cell (after Jaeger and Rosengren, 1969).

4.7.2 Influence of surface roughness on shear strength

Shear tests carried out on smooth, clean discontinuity surfaces at constant normal stress generally give shear stress-shear displacement curves of the type shown in Figure 4.35.

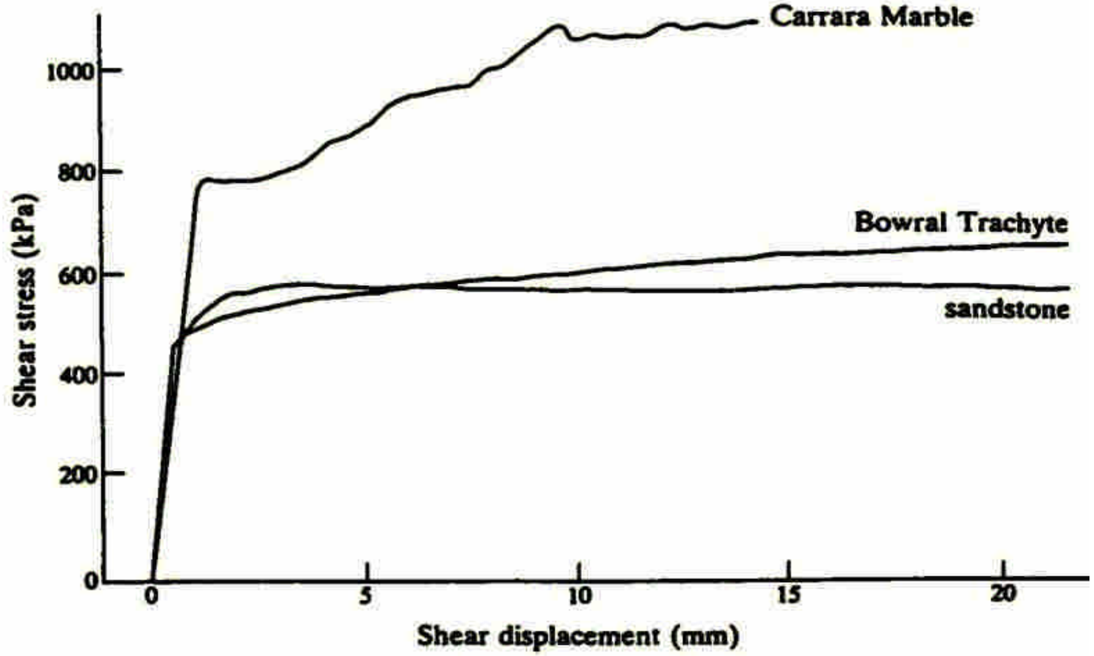

Figure 4.35 Shear stress–shear displacement curves for ground surfaces tested with a constant normal stress of 1.0 MPa (after Jaeger, 1971).